10th INTERNATIONAL SCIENTIFIC CONFERENCE
ON DEFENSIVE TECHNOLOGIES
OTEH 2022
Belgrade, Serbia, 13 – 14 October 2022

NUMERICAL ANALYSIS OF THE TUNGSTEN CARBIDE-COBALT CORED BULLET PENETRATING THE HIGH-HARDNESS STEEL PLATE

RADOVAN ĐUROVIĆ
University of Belgrade, Faculty of Mechanical Engineering, Belgrade, rdjurovic@mas.bg.ac.rs

PREDRAG ELEK
University of Belgrade, Faculty of Mechanical Engineering, Belgrade, pelek@mas.bg.ac.rs

MILOŠ MARKOVIĆ
University of Belgrade, Faculty of Mechanical Engineering, Belgrade, mdmarkovic@mas.bg.ac.rs

DEJAN JEVTIĆ
University of Belgrade, Faculty of Mechanical Engineering, Belgrade, djevtic@mas.bg.ac.rs

MIHAILO ERČEVIĆ
Prvi Partizan, Užice, mihailo.ercevic@prvipartizan.com

Abstract: *In the present study, penetration of a 6.5 mm Grendel armor-piercing projectile with a front tungsten carbide-cobalt core and rear lead-antimony core into the 8.5 mm PROTAC 500 high-hardness armor steel plate was analyzed both experimentally and numerically. Ballistic tests were performed in which the projectile's initial velocity had the value of 740 m/s. Experimental results have shown that the partial perforation with the projectile embedment was the most frequent outcome. Two-dimensional axisymmetric non-linear numerical model corresponding to the performed tests was developed in ANSYS AUTODYN software using the mesh based Lagrangian technique. Johnson-Cook strength and failure models were employed for the characterization of the material behavior. Developed numerical model was verified against the experimental results and the influence of the projectile's impact velocity on the parameters of the penetration was investigated. Rear lead alloy core was found to be able to provide significant enhancement of the projectile's efficiency.*

Keywords: *terminal ballistics, armor-piercing projectile, tungsten-carbide-cobalt, numerical analysis*

1. INTRODUCTION

Small-arms armor-piercing (AP) ammunition is widely used for the perforation of light-armored targets owing to its high penetration efficiency. However, advances in the armor material technology and in the design of protective structures induce a continuous demand for the enhancement of the AP projectiles' ballistic properties.

It is known that increase in the impact velocity has the beneficial effect on the penetration efficiency which, for example, may be seen in the well-known models of Recht and Ipson [1] and Lambert and Jonas [2], and in numerous experimental studies. In order to increase the projectile's impact velocity and kinetic energy, it is necessary to increase projectile's initial velocity and/or to reduce velocity drop over the distance. During the development of the 6.5 mm Grendel bullet, both the gunpowder mass and the projectile's ballistic coefficient were optimized, resulting with the improvement in the bullet's internal and external ballistic properties. In an experimental research [3], performance of the 6.5 mm Grendel bullet was compared with that of the 5.56x45 mm SS109 and the 7.62x39 mm API bullets. Their velocities were measured over the range of 700 meters and based on the obtained results, it was concluded that the projectile's kinetic energy is by far the highest in the case of 6.5 mm Grendel cartridge, exceeding that of the 7.62x39 mm for more than double on the medium and long ranges. Nevertheless, even though the increase in kinetic energy may provide increase in penetration, it may also lead to the loss of the projectile's integrity due to the high values of compressive and bending loads being exerted on it during the ballistic impact. Thus, it is highly important to conduct a thorough investigation of the projectile-target interaction which for the high velocity impacts may be done through experimental, analytical and numerical approaches [4]. Numerical simulations have shown to be a valuable tool in the design phase as their usage can lead to the shorter development time and to the reduced number of prototypes and ballistic tests, while providing accurate prediction of the complex physical phenomena during the ballistic impacts.

In the present study, ballistic testing of the 6.5 mm Grendel armor-piercing tungsten carbide-cobalt (WC-Co) cored projectile against PROTAC 500 high-hardness armor steel was conducted and corresponding two-dimensional numerical model was developed in the ANSYS AUTODYN software. Accuracy and utility of the

numerical models in the field of penetration mechanics are usually limited by the material behavior description [5], thus making it necessary to validate the developed model against the obtained experimental results. In the process of model validation, influence of the rear lead alloy core and its erosion criteria value on the penetration process was investigated. After the good agreement between the experimental results and the numerical model was achieved, additional simulations with the different values of impact velocities were conducted.

2. BALLISTIC TESTS

In a series of ballistic tests, 6.5x39 mm Grendel armor-piercing rounds (Fig. 1) were fired through a 415 mm long ballistic test barrel into the 8.5 mm thick PROTAC 500 high-hardness steel plate. Square-shaped plate with the edge size of 500 mm was mounted in the rigid frame and placed at the distance of 100 meters from the barrel muzzle. In order to enhance the credibility of the tests and to assure no reciprocal influence in the results, in-plane distance between adjacent shots and the boundaries was kept greater than 100 mm [6]. During the tests, angle of incidence between the projectile and the target plate was kept normal.

In total, nine tests with the bullet's nominal initial velocity of 740 m/s were conducted. Its value was being monitored with the use of the infrared optical velocity measuring system. Based on the measured values and on the known projectile's ballistic coefficient of 0.540 (G1 drag function), the impact velocity was calculated and its average value was found to be equal to 702.1 m/s. Deviations from the average value were found to be minor and negligible. HPI B590 optical target system was used for the acquisition of the projectile's accuracy data.

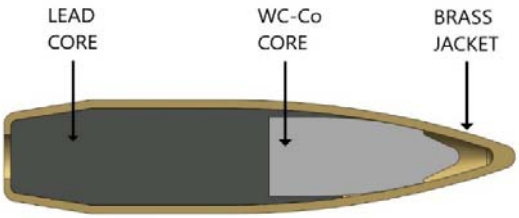

Figure 1. Cross-section of 6.5 mm Grendel AP projectile

As it may be seen in Fig. 1, observed armor-piercing projectile consists of front tungsten carbide-cobalt core and rear lead-antimony core which are both being encased in the brass jacket. Hard WC-Co core has the mass of 1.8 grams with the length of 11 mm and the diameter of its cylindrical section equal to 4.7 mm. Mass of the complete projectile is 7.8 grams and its length is 30.2 mm.

Results of the conducted firings have shown that the complete perforation wasn't achieved in any of the tests. In seven firings, partial perforation with the penetrator embedment was observed, while in the two firings no perforation was observed at all. Pictures of several distinct penetration process outcomes may be seen in Fig. 2. For the great majority of the conducted firings, ductile hole formation in initial stage and adiabatic shear plugging in the second stage of penetration was observed as the failure mechanism. Due to the fact that shear bands nucleate and propagate to the rear surface independently, plugging failure will generally lead to the asymmetric deformation and combination of adiabatic shear with the bending away and fracture of the plug from the target [7]. Side views in Fig. 2 clearly indicate that in the firings without the perforation (labeled A and B), the adiabatic shear plugging with the asymmetric plug formation had occurred but that the fracture and consequent ejection of the plug failed to happen. Inspection of the indentations created during those impacts has shown that the penetrator wasn't embedded in the target plate, indicating that its fragmentation had occurred during the process of penetration due to the high loads. Collapse of the penetrator material was also observed in several firings in which the partial perforation has been achieved (D in Fig. 2). Initial stage of penetration was identified as critical, as during this stage the core undergoes the maximum compressive and bending loads which often cause the collapse of the WC-Co composite due to its brittleness [8]. Frontal conical section of the WC-Co penetrator has shown to be particularly susceptible to the exerted loads, while the cylindrical section stayed intact and was found embedded in the target plate. In lesser number of firings, the whole penetrator was found intact and embedded in the target plate (C in Fig. 2).

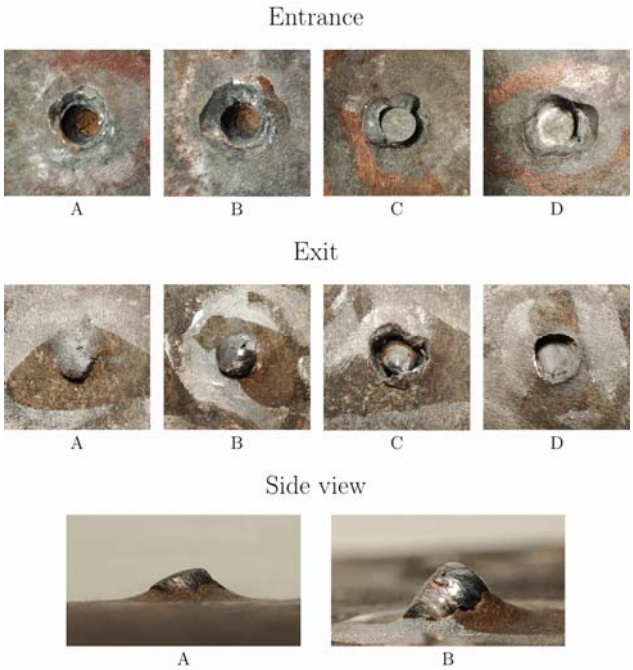

Figure 2. Target plate damage morphology

No evidence of the lead-antimony core and brass jacket embedment was recorded, indicating their complete destruction in the process of penetration. However, their influence may be seen in the zone of the hole entrance where the cratering was observed for all of the conducted firings. This behavior is characteristic in the penetration of metallic targets with a cored projectile that is achieved via the ductile hole formation mechanism [9]. On the rear surface of the target plate, bulges have been formed in

seven firings with partial perforation outcome. Their maximum heights were in the range from 1.1 to 1.8 mm while the diameters of the generated holes were in the range from 4.5 to 4.9 mm. Plugs created during the two firings without the achieved perforation have the maximum height of 2.2 mm (A in Fig. 1) and 3.6 mm (B), measured from the rear surface of the target.

Differences observed in the outcomes of the performed firings can be attributed to the stochastic nature of ballistic tests. During the research of Kilic et al. [10], it was found that only one of five shots has shown the perpendicular intrusion in the target material while in the remaining impacts the obliquity was detected. Based on the analysis of the target plate after the ballistic tests were performed, similar conclusion was made in the present research.

3. MATERIAL MODELS

High velocity impacts and penetrations are exceptionally complex processes and their numerical modeling represents a great challenge due to the occurrence of high strain-rates, large deformations, high temperatures etc. which make the characterization of material behavior and failure difficult. One of the most widely used constitutive models was developed by Johnson and Cook [11]. It is an empirical visco-plastic model which is suitable for the modeling of ductile metals and which takes into account strain hardening, strain rate and thermal softening effects. According to it, the equivalent stress may be expressed as:

$$\sigma_Y = \left[A + B\varepsilon_p^n\right]\left[1 + C\log\dot{\varepsilon}_p^*\right]\left[1 - T_H^m\right] \quad (1)$$

where ε_p is the equivalent plastic strain, $\dot{\varepsilon}_p^*$ is the dimensionless plastic strain rate for $\dot{\varepsilon}_0$, T_H is homologous temperature $\mathrm{T_H} = (\mathrm{T} - \mathrm{T_{room}})/(\mathrm{T_{melting}} - \mathrm{T_{room}})$, while A, B, C, n and m are material constants.

Apart from the material strength model, Johnson and Cook have also developed a ductile failure model which takes into account effects of strain rate, temperature and stress triaxiality on failure strain [12]. According to it, failure strain for metals increases with increase in temperature, while it decreases with increase in strain rate and stress triaxiality. The Johnson-Cook failure model is empirical cumulative damage – fracture model which assumes that damage is accumulated in the material during the plastic straining until a critical value is reached after which the material breaks immediately. Thus, the damage has no contribution on the stress field until the fracture occurs. Due to the J-C model being an instantaneous failure model, no strength of eroded material elements will remain after their erosion happens.

The damage to an element is defined by:

$$D = \sum \frac{\Delta\varepsilon}{\varepsilon^f} \quad (2)$$

where $\Delta\varepsilon$ is the increment of equivalent plastic strain and ε^f is the equivalent strain to fracture given by:

$$\varepsilon^f = \left[D_1 + D_2\exp(D_3\sigma^*)\right]\left[1 + D_4\ln\left|\dot{\varepsilon}_p^*\right|\right]\left[1 + D_5 T_h\right] \quad (3)$$

Material parameters D_1, D_2 and D_3 which represent the strain hardening are predominant when compared with two other which represent the strain rate hardening (D_4) and thermal softening (D_5). The dimensionless pressure-stress ratio σ^* represents a measure of stress state triaxiality. The damage variable D may take values in a range from 0 to 1 where $D = 0$ represents undamaged material elements while in the elements in which D reaches 1 the fracture will occur, leading to their removal from the simulation. In order to implement the Johnson-Cook strength and fracture models in the numerical analysis, it is necessary to know the material parameters. PROTAC 500 was experimentally and numerically investigated in the study of Trajkovski et al. [13]. Its J-C model parameters were determined and are given in table 1, together with basic mechanical properties.

Table 1. PROTAC 500 basic mechanical properties and Johnson-Cook parameters [13]

Density			7.85 g/cm³		
Hardness			470-540 HB		
Yield strength			1400 MPa		
Tensile Strength			1800 MPa		
Elongation A5			10 %		
Strain hardening			Strain rate hardening		Temperature softening
A [MPa]	B [MPa]	n	c	$\dot{\varepsilon}_0$ [s^{-1}]	m
1380	948	0.2351	0.0035	0.001	1.087
D_1	D_2	D_3	D_4	$\dot{\varepsilon}_0$ [s^{-1}]	D_5
0.0001	1.586	-1.718	0.00695	0.001	3.247

Lead being used for the production of bullet cores is generally alloyed with antimony with the aim to increase its hardness and strength [14]. Antimony content can range from 0.5 to 25 wt.-% and in the present study, it was equal to 8 wt.-%. Brass from which the jacket is made is widely used CuZn10 alloy, also known as red brass and tombac. Mechanical properties of both the lead alloy and the brass are relatively low when compared with those of tungsten carbide-cobalt and high hardness armor steel. Thus, severe deformation and distortion will appear in the jacket and soft core elements during the high-velocity impact. In order to avoid simulation interruption, Lagrange solver relies on a technique of numerical erosion for the deletion of highly strained elements. Several erosion criteria are available in AUTODYN software, including the erosion upon material failure and instantaneous geometric strain erosion. Johnson-Cook failure model was used as erosion criteria for brass, while in the case of lead alloy a preliminary value of 2.5 was chosen for the instantaneous geometric strain erosion [15]. Even though the latter one represents an ad hoc method that has no physical basis, knowledge of the ballistic test outcome makes it possible to determine the appropriate erosion criteria and the erosion strain value. In Table 2, Johnson-Cook model parameters for the jacket and the soft core materials are summarized.

Table 2. Johnson-Cook parameters for lead alloy and brass

Lead core [16]					
Strain hardening			Strain rate hardening		Temperature softening
A [MPa]	B [MPa]	n	c	$\dot{\varepsilon}_0$ [s^{-1}]	m
10.3	41.3	0.21	0.00333	0.01	1.03
Brass jacket [16]					
Strain hardening			Strain rate hardening		Temperature softening
A [MPa]	B [MPa]	n	c	$\dot{\varepsilon}_0$ [s^{-1}]	m
448.2	303.4	0.15	0.00333	0.01	1.03
D_1	D_2	D_3	D_4	$\dot{\varepsilon}_0$ [s^{-1}]	D_5
2.25	0.0005	-3.6	-0.0123	0.01	0

Materials for armor-piercing projectiles' hard cores are often modeled as rigid, due to their high mechanical properties [17]. Tungsten carbide-cobalt (WC-Co) is a metal-ceramic composite characterized by high hardness, high density and relatively good compressive and bending strength values [8]. In the present study, WC-Co alloy (85% WC, 15% Co) with a hardness of 1090 HV and density of 14.08 g/cm^3 was used as the core material and in the conducted simulations it was modeled as rigid.

4. NUMERICAL MODEL

Two-dimensional axisymmetric model corresponding to the conducted ballistic test was developed in ANSYS AUTODYN. Mesh based Lagrangian technique was employed during the model development as it is computationally efficient and provides insight into the material boundaries. Its downside is that it requires implementation of element erosion in order to handle severe mesh distortions which will inevitably appear during the ballistic impact simulations. Deletion of highly deformed cells will lead to the removal of internal material energy from the model which will result in reduced accuracy. Apart from the WC-Co penetrator that is modeled as rigid, other parts of the projectile and the target are prone to the element erosion and loss of internal energy, with the jacket and lead core being exceptionally susceptible to it as they are made from ductile materials which undergo large deformations during the penetration process. However, as it was concluded in the work of Borvik et al. [6], ballistic limit velocity was reduced by 3 to 5 % when only the hard core of the projectile was used indicating that the effect of the brass jacket and the lead cap on the penetration process is minor. Thus, it was concluded that the Lagrangian discretization may be used in the present research. Nevertheless, due to the large volume and mass of the lead alloy core when compared to the WC-Co core, additional simulations were conducted with the hard core as the only element of the projectile.

During the experiment, target plate with the impact area of 500x500 mm was used. However, in order to reduce the computational cost of the simulation target was modeled as a circular, axisymmetric plate with the radius of 100 mm which corresponds to the distance between adjacent shots. As the projectile's dimensions are considerably smaller when compared to the target radius, finer mesh was created in the central zone of the target plate and as a result, element size gradually increases in radial direction from 0.1 mm in the zone of impact to the 0.5 mm at the target's outer surface where the fixed boundary condition was applied. Element size in range from 0.1 mm to 0.15 mm was chosen for the meshing of the projectile and in total, around 26000 elements were formed for the purpose of target and projectile discretization. Created Finite Element model may be seen in Fig. 3, where the 2D model was rotated for 90° about the symmetry axis in order to provide a better representation of the model's geometry. Only a central zone of the target is shown due to its large radius.

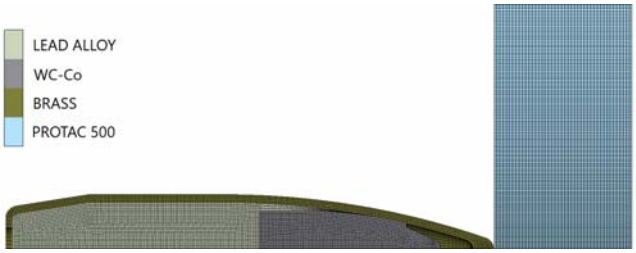

Figure 3. FE model of the projectile and the target

Geometry of the projectile's numerical model is identical to the geometry of the actual bullet. For the purpose of model validation, impact velocity and target thickness were same as in the ballistic test. Friction between the projectile and target was neglected as its influence is considered to be minor in the high velocity impacts.

5. RESULTS AND DISCUSSION

Using the presented numerical model, a simulation corresponding to the conducted experimental firings was performed. Furthermore, an additional simulation was conducted in which the brass jacket and the lead core were removed, thus making it possible to determine the degree of their influence on the penetration process parameters. As a result, profiles of WC-Co core's velocity over time (Fig. 4) and vs. its displacement (Fig. 5) were created for both of the observed cases. Reference coordinate system was set at the target plate's impact surface and the displacement of the hard core was measured from it after the contact with the target was achieved. For a better understanding of the presented velocity curves, a sequence of plots displaying the evolution of the penetration process is shown in Fig. 6.

In the simulation with the complete projectile, WC-Co core had to penetrate through the jacket tip (as it may be seen in plot for $t = 4.13\ \mu s$ in Fig. 6), thus experiencing a drop in velocity prior to its contact with the target at $t = 4.78\ \mu s$. However, by comparing the results from both of the conducted simulations it was found that the difference in velocity caused by this drop is less than 1%, indicating that the brass jacket may be neglected.

Furthermore, it may be seen in Fig. 6 that the erosion of the jacket material happens with almost no damage being generated in the target plate which additionally confirms the previously stated conclusion. On the other hand, numerical results show that the influence of the lead alloy core is significant and that it may not be neglected due to the great differences in the penetration process parameters which have been observed.

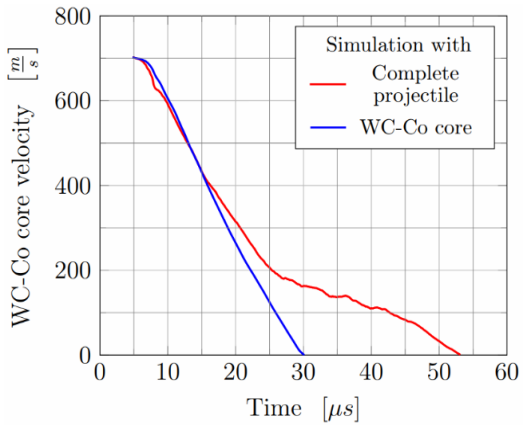

Figure 4. WC-Co core's velocity over time for the simulations with the complete projectile and with the WC-Co core only

Upon the impact of the WC-Co core into the target plate and throughout the penetration, significant change of the velocity was observed in both of the simulations. However, character of that change greatly differs during the majority of the penetration process. Velocity vs. time curve for the simulation with only the WC-Co core has a steep gradient with the approximately constant value of the deceleration. Observed curves are similar only during the first 10 μs of the penetration, from the moment of impact to around 15 μs where they start diverging. This point represents the end of the first out of four sections which can be seen on the velocity vs. time curve for the complete projectile simulation. Second section is characterized by an increase in the slope and the decrease in deceleration by 31.8%. However, its value is still relatively high causing further velocity drop, although more moderate than in the case with the WC-Co core as the only part of the projectile.

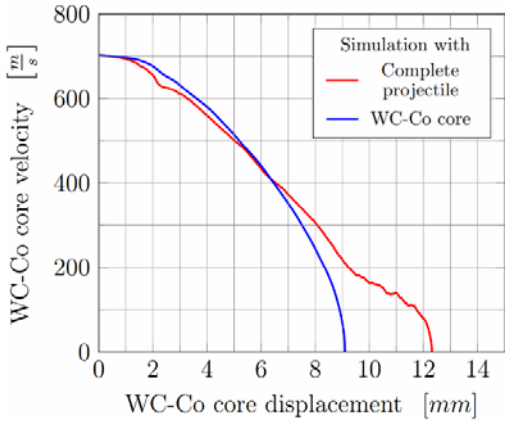

Figure 5. WC-Co core's velocity vs. displacement for the simulations with the complete projectile and with the WC-Co core only

Simulation results have shown that first two sections are responsible for the majority of the WC-Co core's penetration. In fact, 9.1 mm or 74% of the core's total axial displacement of 12.3 mm had been accomplished during them while the first section alone is accountable for the 48.8% of the core's total displacement (Fig. 5). By observing the plots for t = 8.56 μs and t = 16.37 μs shown in Fig. 6, it may be seen that during the first section there was no significant erosion of the lead alloy core. Thus, it may be concluded that the WC-Co core is able to provide relatively large penetration even though its mass represents only 23% of the complete projectile's mass. However, enhancement of the WC-Co core's penetration by the effect of the lead alloy core is significant and clearly visible, especially in the third section during which the additional displacement equal to 3.2 mm is achieved. In the observed case, 26% of the WC-Co core's total axial displacement may be attributed to the lead alloy core.

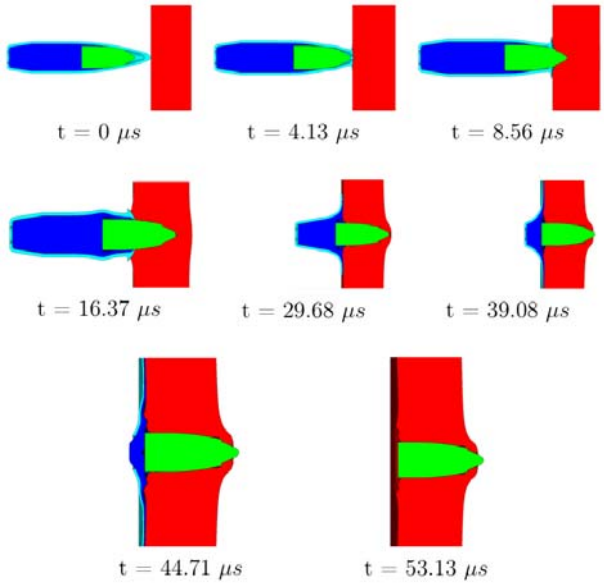

Figure 6. Evolution of the penetration process in the simulation corresponding to the performed experiment

Velocity drop during the third section is also heavily influenced by the lead alloy core, resulting in the considerably smaller deceleration. End of the this section is characterized by the complete erosion of the lead core that had occurred at around 46 μs. Even though the WC-Co core still had a velocity of around 80 m/s in that moment, it was not be able to provide any additional displacement during the fourth section (Fig. 5).

Based on the experimental results, it was concluded that the simulation with the complete projectile had provided better agreement than that with hard core only. Partial perforation with the projectile embedment was achieved which is in accordance with the majority of the conducted ballistic tests. Furthermore, a comparable value of penetration depth was achieved as in Fig 2, case C. Minor deviation between the model and the experiment may be seen on the target's impact surface where the crater created during the simulation is considerably smaller in both the depth and the diameter than the experimental one. Also, ejection of the target plate's material from its rear surface wasn't reproduced properly. However, this

may be attributed to the changes in the material failure mechanisms between the initial and second stage of penetration and the transition from the ductile to brittle failure which may not be described accurately using the same material model. Ductile hole formation during the initial stage of the penetration was, on the other hand, successively simulated.

Due to the conclusion that the lead core may not be neglected, additional simulations have been performed with the values of erosion strain (ES_{IGS}) different from the preliminary value of 2.5 as the calibration of this erosion criteria against the experimental results had to be done. Velocity and displacement histories for those simulations may be seen in Fig. 7. Acquired results have shown that the velocity vs. time curves significantly differ only in the fourth section and that the crucial changes in the hard core's displacement weren't observed. Best agreement with the experiment may be achieved with the ES_{IGS} values in range from 2.3 to 2.5 and in the following simulations, numerical model with the erosion strain of 2.5 was used.

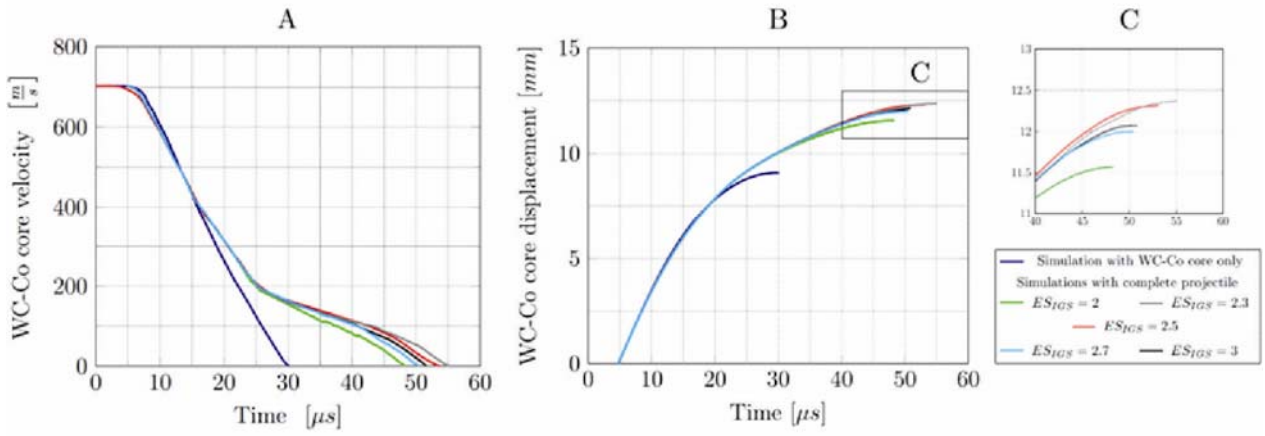

Figure 7. Velocity (A) and displacement (B) of the WC-Co core over time for the several values of ES_{IGS} erosion strain in the range from 2 to 3

Experimental results shown in Section 2 indicate that the observed impact velocity is in vicinity of the ballistic limit velocity for the observed projectile and target plate configuration. In order to determine the change in the parameters of the penetration process under the different impact velocities, additional numerical simulations were performed using the previously described and verified numerical model. WC-Co core's velocity vs. displacement curves for the impact velocities in range from 660 m/s up to 770 m/s are displayed in Fig. 8. In accordance with the obtained results, the projectile will be able to achieve complete perforation of the target under the impact velocities equal to 730 m/s and higher. Significant change in the value of residual velocity was observed even with the small increase in the impact velocity. This can be partially attributed to the observed change in the influence of the lead alloy core during the third section of penetration. As it may be seen in Fig. 8, value of the WC-Co core's velocity at which the third section starts increases greatly with the increase in impact velocity and that is accompanied with the increased slope for that section. This increase in the slope can even result in the positive value being achieved, meaning that the increase in the WC-Co core's velocity caused by the contribution of the lead core surpasses the decrease caused by the resistance of the target plate. Thus, velocity of the hard core may even increase during the penetration.

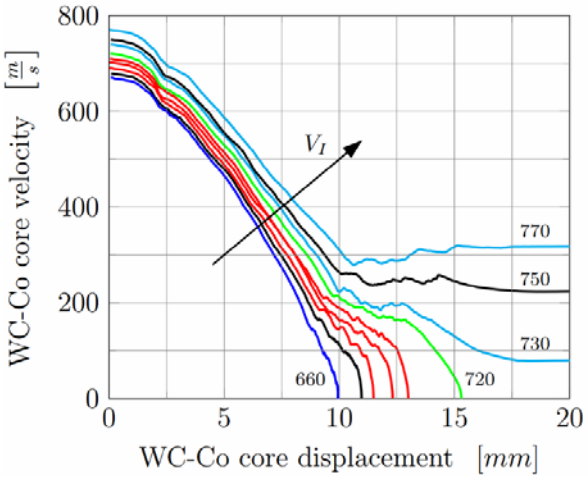

Figure 8. WC-Co core's velocity vs. displacement for the several values of the projectiles impact velocity V_I

Decrease in the value of the impact velocity will result in the increased deceleration in the third section; in the reduction of its duration and in the reduced contribution of the lead alloy core to the total axial displacement. For the lowest impact velocity considered in the present study, third section had almost been blended into the second section and the penetration achieved during it has been minimized. This may pose a risk to the efficiency and usability of the observed projectile on the mid and long ranges where a considerably lower values of impact velocities are to be expected. On the other hand, implementation of the rear core made from lead alloy had led to the significant enhancement of the projectile's ballistic properties in the cases of impact velocities above

the ballistic limit and this may be valuable on the short ranges. Main advantage of the lead is that is highly ductile when compared to the brittle tungsten carbide-cobalt alloy. By the utilization of the presented dual core configuration, same level of penetration could be achieved with the WC-Co core that is smaller in size and thus, less prone to the loss of integrity during the penetration process.

5. CONCLUSIONS

Ballistic tests and two-dimensional numerical simulations have been performed with the aim to investigate the high velocity impact of the dual-cored 6.5 mm Grendel AP projectile into the 8.5 mm thick high hardness steel plate. Some of the important conclusion and observations are:

- Experimental firings have shown that the partial perforation with the projectile embedment was the most common penetration process outcome. Also, in two out of nine firings perforation was not achieved at all indicating that the impact velocity is close to the ballistic limit velocity. During the tests, obliquity angle was kept normal and the average value of the projectile's impact velocity was 702.1 m/s. Tungsten carbide-cobalt core had lost its integrity in majority of the tests which can be attributed to its brittleness and the high compressive loads exerted on it during the penetration process. Ductile hole enlargement was identified as the main failure mechanism,
- Numerical model developed in ANSYS AUTODYN using the Lagrangian mesh based technique was able to provide a good agreement between the numerical and experimental results. WC-Co core was modeled as rigid while the other elements of the projectile and the target were modeled using the Johnson-Cook strength and failure models, with the exception of lead alloy core where the instantaneous geometric strain was applied as the failure and erosion criteria.
- Calibration of the erosion strain value was conducted against the experimental results by performing the simulations with the ES_{IGS} values in range from 2 to 3. With the exception of the lowest considered value, others were found to produce a similar outcome and the differences in the velocity and displacement curves between them were relatively small. However, best agreement was provided by the values of 2.3 and 2.5 and the latter one was adopted as the erosion strain value for the developed numerical model.
- Simulation results have shown that the brass jacket has a minor influence on the parameters of the penetration process and that it may be neglected. On the contrary, influence of the lead alloy core was found to be significant and non-negligible. For the simulation corresponding to the conducted firings, soft core was solely responsible for the 26% of the hard core's total axial displacement. Beneficial effects provided by the lead alloy core were found to increase with the increase in the projectile's impact velocity. For the values that are far enough from the BLV, WC-Co core's velocity even grew in value during one part of the penetration. However, even a small decrease in the value of impact velocity had strongly reduced the projectile's penetration which may pose a threat to its efficiency and utility on the mid and long ranges.
- Although good agreement was achieved with the rigid model of the WC-Co, additional effort needs to be made in the implementation of the deformable model that will successfully model brittleness and failure.

References

[1] RECHT, R., IPSON, T.: *Ballistic perforation dynamics,* Journal of Applied Mechanics*, 30, (1963)*

[2] LAMBERT, J., JONAS, G.: *Towards standardization in terminal ballistics testing: velocity representation,* U.S. Army Ballistic Research Laboratory, (1976)

[3] JOKIĆ, Ž. ET AL.: *Primena VIKOR metode prilikom izbora kalibra za automatske puške u cilju uvođenja u operativnu upotrebu u jedinicama Vojske Srbije*, Vojno delo, 71(6), (2019), 200-221

[4] ZUKAS, J.: *Introduction to Hydrocodes,* Elsevier Science, (2004)

[5] ZUKAS, J. ET AL.: *Impact dynamics,* Wiley, (1982)

[6] BORVIK, T. ET AL.: *Perforation resistance of five different high-strength steel plates subjected to small-arms projectiles,* International Journal of Impact Engineering, 36, (2009), 948-964

[7] WOODWARD, R.: *The interrelation of failure modes observed in the penetration of metallic targets,* International Journal of Impact Engineering, 2, (1984), 121-129

[8] KOLMAKOV, A. ET AL.: Materials for Bullet Cores, Russian Metallurgy (Metally), (2021), 351-362

[9] ME-BAR, Y.: *On the correlation between the ballistic behavior and dynamic properties of titanium-alloy plates,* International Journal of Impact Engineering, 19, (1997), 311-318

[10] KILIC, N.: *Ballistic resistance of high hardness armor steels against 7.62 mm armor piercing ammunition,* Materials and Design, 44, (2013), 35-48

[11] JOHNSON, G., COOK, W.: *A constitutive model and data for metals subjected to large strains, high strain rates and high temperatures,* Proceedings of the 7th international symposium on ballistics, (1983)

[12] JOHNSON, G., COOK, W.: *Fracture characteristics of three metals subjected to various strains, strain rates, temperatures and pressures*, Engineering Fracture Mechanics, 21, (1985), 31-48

[13] TRAJKOVSKI, J. ET AL.: *Flow and fracture behavior of high-strength armor steel PROTAC 500*, Materials and Design, 66, (2015), 37-45

[14] PERONI, L. ET AL.: *Mechanical properties at high strain-rate of lead core and brass jacket of a NATO 7.62 mm ball bullet,* The European Physical Journal Conferences, 26, (2012)

[15] TELAND, JAN: *Numerical Simulation of Light Armor-Piercing Ammunition Against Ceramics*, Norwegian Defence Research Establishment, (2004)

[16] CARBAJAL, L. ET AL.: *Assault Rifle Bullet-Experimental Characterization and Computer (FE) Modeling,* Experimental and Applied Mech., (2011)

[17] MANES, A. ET AL.: *Ballistic performance of multi-layered fabric composite plates impacted by different 7.62 mm caliber projectiles,* Procedia Engineering, 88, (2014)